Symplectic Integrator Algorithms for Modelling Planetary Accretion in Binary Star Systems

John E. Chambers

Space Sciences Division 245-3, NASA Ames Research Center, Moffett Field, CA 94035;

john@mycenae.arc.nasa.gov

Elisa V. Quintana

Space Science Division 245-3, NASA Ames Research Center, Moffett Field, CA 94035

and Department of Physics, University of Michigan, Ann Arbor, MI 48109;

equintan@estrellas.arc.nasa.gov

Martin J. Duncan

Department of Physics, Queen's University, Kingston, ON K7L 3N6, Canada;

duncan@astro.queensu.ca

Jack J. Lissauer

Space Science Division 245-3, NASA Ames Research Center, Moffett Field, CA 94035;

jlissauer@ringside.arc.nasa.gov

Received _____; accepted _____

ABSTRACT

We derive and test two new symplectic integrator algorithms, suitable for studying planetary accretion in binary star systems. The algorithms incorporate the hierarchical nature of stable planetary orbits in binary star systems. In one case, planets orbit a single star, perturbed by a distant companion; in the second case, planets orbit both binary members. Each algorithm integrates close encounters between planets symplectically using a hybrid symplectic scheme.

Subject headings: celestial mechanics, stellar dynamics—methods: n-body simulations—methods: numerical

1. Introduction

N-body symplectic mapping techniques are the tool of choice for many problems that require high speed, moderately accurate N-body integrations. These algorithms (also referred to as mixed-variable symplectic integrators, after Saha and Tremaine 1992) were introduced by Wisdom and Holman (1991) and Kinoshita *et al.* (1991). They have since been used to tackle a wide variety of problems in Solar System dynamics, planetary and satellite accretion, and extrasolar planetary systems (*e.g.*, Levison & Duncan 1994, Chambers & Wetherill 1998, Canup *et al.* 1999, Rivera & Lissauer 2000).

Symplectic algorithms have two big advantages over other methods. First, for problems involving a dominant central mass, the Keplerian motion of the satellites about the primary is "built in". As a result, most of the computational effort is devoted to the perturbations between the satellites, which makes it possible to use long timesteps with many fewer force evaluations than conventional algorithms such as Bulirsch-Stoer (Stoer and Bulirsch 1980) or RADAU (Everhart 1985). As a rule of thumb, this gives the symplectic algorithms a speed advantage of about an order of magnitude for problems that do not require very high accuracy solutions. The second advantage of symplectic schemes is that they exactly follow the evolution of a Hamiltonian system, albeit one that is not exactly the same as the real system. This means that, except for numerical roundoff error, they exhibit no long-term build up in energy error.

Recently, Duncan *et al.* (1998) and Chambers (1999) have described how to modify the basic symplectic scheme to cope with situations in which perturbations between satellites are no longer small compared to the force due to the primary. This makes it possible to integrate close encounters between bodies, and to model planetary or satellite accretion. The two modified algorithms differ in design, but appear to give comparable results in practice, and each retains the advantages of the original method.

To date, one problem which has not been examined using symplectic integrators is planetary accretion in binary star systems. The discovery of extrasolar planets in binary systems (*e.g.*, Cochran *et al.* 1997), and the fact that most stars in the galaxy are part of such systems, makes this a worthwhile problem for study. At first sight, symplectically integrating planetary orbits in binary systems presents a problem since the usual rationale for symplectic methods is based on the fact that a system contains a single dominant body and not two. However, all long-lived planetary systems involving binary stars are likely to be hierarchical—either the planets orbit the center of mass of a pair of stars of small separation; or the planets orbit one star, and the second star orbits at a considerably larger distance. The hierarchical nature of these systems makes it possible to modify the earlier symplectic schemes, while still permitting close encounters, in order to perform realistic planetary accretion simulations in binary star systems. In this paper we describe how to modify the *Mercury* hybrid-symplectic algorithm of Chambers (1999), but we note that similar modifications could be easily applied to the SyMBA algorithm of Duncan *et al.* (1998).

The rest of this paper is organized as follows. Section 2 contains a brief review of the theory of symplectic integrators, and their modification to include close encounters. In Section 3, we describe how the algorithms can be adapted to follow orbits in each type of hierarchical binary systems. Finally, Section 4 describes tests we have made using the new schemes.

2. Symplectic Integrators Based on N-body Mappings

For a Hamiltonian system of N bodies with Hamiltonian H, the rate of change of any quantity q can be expressed using

$$\frac{dq}{dt} = \sum_{i=1}^{3N} \left(\frac{\partial q}{\partial x_i}\frac{\partial H}{\partial p_i} - \frac{\partial q}{\partial p_i}\frac{\partial H}{\partial x_i} \right) = Fq, \tag{1}$$

where F is a differential operator, and $(\mathbf{x}_i, \mathbf{p}_i)$ are the coordinates and momenta of body i. This equation has a formal solution

$$q(\tau) = e^{\tau F} q(0) = \left(1 + \tau F + \frac{\tau^2 F^2}{2} + \cdots \right) q(0), \tag{2}$$

where τ is a short interval of time.

In celestial mechanics problems, H can often be split into two or more pieces, so that each part of the problem can be solved easily in the absence of the other. For example, if H is split into two pieces, H_A and H_B, we can associate each piece with a new differential operator, A and B, by analogy with F. In this case, the solution for q becomes

$$q(\tau) = e^{\tau(A+B)} q(0). \tag{3}$$

Symplectic integrators can be designed by replacing the exponential term above with a series of terms in $\exp \tau A$ and $\exp \tau B$, such that their product is approximately equal to $\exp \tau(A + B)$. For example, the popular second-order "leapfrog" integrator is given by

$$e^{\tau B/2} e^{\tau A} e^{\tau B/2} q(0) = q(\tau) + O(\tau^3). \tag{4}$$

If we think of τ as the stepsize of the leapfrog integrator, then one timestep consists of calculating the evolution of the initial conditions under H_B for a time $\tau/2$, then advancing the resulting system under H_A for a time τ, then advancing the result under H_B for time $\tau/2$. The end product is equivalent to the evolution of q in the real problem with an error proportional to τ^3. Leapfrog is a low order integrator, meaning that in general a very short stepsize is required to give accurate results.

The great speed advantage of symplectic algorithms comes from choosing H_A and H_B so that the latter is much smaller than the former by a factor $\epsilon \ll 1$. In this case the error

per timestep becomes $O(\epsilon\tau^3)$, and thus a much larger stepsize can be used to achieve the same level of accuracy as the general case. The usual way this is done is to associate H_A with the Keplerian motion of satellites about the primary, and H_B with the mutual forces between satellites and other small perturbations. For hierarchical systems in which close encounters do not occur (*e.g.* the planets in the Solar System), Wisdom and Holman (1991) recommend using Jacobi coordinates, in which satellites are ordered according to their distance from the primary, and coordinates are measured relative to the center of mass of all bodies with smaller indices. Advancing H_A and H_B using Jacobi coordinates is a somewhat complicated business, but the method is described in detail in Saha and Tremaine (1994).

Close encounters between satellites pose a problem because during an encounter it is no longer true that $H_B \ll H_A$. Hence ϵ increases, and the error per timestep can become large enough to render an integration useless unless the timestep is initially chosen to be very small (which of course defeats the speed advantage of the symplectic algorithms). Duncan *et al.* (1998) and Chambers (1999) describe two ways to overcome this problem, but in each case Jacobi coordinates turn out to be an inefficient choice. Both sets of authors advocate using what the former have called "democratic heliocentric" (DH) coordinates, in which satellite positions are measured with respect to the primary, while satellite velocities are measured with respect to the center of mass of the whole system.

Using DH coordinates, the Hamiltonian for a system of N satellites orbiting a primary is given by $H = H_A + H_B + H_C$, where

$$\begin{aligned} H_A &= \sum_{i=1}^{N} \left(\frac{p_i^2}{2m_i} - \frac{Gm_0 m_i}{r_{i0}} \right), \\ H_B &= -G \sum_{i=1}^{N} \sum_{j=i+1}^{N} \frac{m_i m_j}{r_{ij}}, \\ H_C &= \frac{1}{2m_0} \left| \sum_{i=1}^{N} \mathbf{p}_i \right|^2, \end{aligned} \tag{5}$$

where index 0 refers to the primary. Here, H_A is the sum of the Kepler motions of each satellite, H_B is the sum of the direct interactions between satellites, and H_C is a set of indirect correction terms. In the absence of close encounters, both H_B and H_C are small compared to H_A. Because H now consists of 3 pieces, the leapfrog integrator of Eq. (4) becomes

$$e^{\tau B/2} e^{\tau C/2} e^{\tau A} e^{\tau C/2} e^{\tau B/2} q(0) = q(\tau) + O(\tau^3), \tag{6}$$

where C is a new differential operator associated with H_C.

Chambers (1999) solves the close-encounter problem by partitioning each of the terms in H_B between H_A and H_B, such that the part in H_B is always small, while the part in H_A goes to zero except during a close encounter:

$$H_A = \sum_{i=1}^{N} \left(\frac{p_i^2}{2m_i} - \frac{Gm_0 m_i}{r_{i0}} \right) - G \sum_{i=1}^{N} \sum_{j=i+1}^{N} \frac{m_i m_j}{r_{ij}} [1 - K(r_{ij})],$$

$$H_B = -G\sum_{i=1}^{N}\sum_{j=i+1}^{N}\frac{m_i m_j}{r_{ij}}K(r_{ij}),$$
$$H_C = \frac{1}{2m_0}\left|\sum_{i=1}^{N}\mathbf{p}_i\right|^2. \quad (7)$$

A suitable choice for $K(r)$ is a function that satisfies $K \to 0$ when $r \to 0$, and $K = 1$ when r is not small.

Using this partitioning, ϵ remains small, and the integrator's accuracy is not severely degraded during close encounters. However, some of the terms in H_A are no longer soluble analytically during an encounter (when some of the $K(r_{ij})$ are non zero), and these terms have to be integrated numerically to high accuracy. This can be achieved using a conventional integrator such as Bulirsch-Stoer, and for this reason the algorithm is referred to as a "hybrid symplectic" integrator, although it still retains the properties associated with other symplectic schemes.

3. Symplectic Integrators for Binary Systems

Test particle orbits in binary systems can be integrated with the standard symplectic mapping technique using Jacobi coordinates (*e.g.*, Wiegert and Holman 1997, Holman and Wiegert 1999). However, this method no longer works when close encounters can occur, so we need to find a new method which can incorporate the special close-encounter procedures used by Duncan *et al.* (1998) or Chambers (1999). There are two possible configurations for planetary orbits in binary star systems: the planets can orbit either one or both members of the binary. Each configuration can treated using a modified symplectic scheme, but the two schemes are different, and we consider the two cases separately in the following sections.

3.1. Wide Binary

In a wide binary, two stars move on widely separated orbits, and in many cases it is possible for long-lived planetary orbits to exist around one of the stars (Holman and Wiegert 1999). The Hamiltonian for a system containing N planets is

$$H = \frac{p_A^2}{2m_A} + \frac{p_B^2}{2m_B} + \sum_{i=1}^{N}\frac{p_i^2}{2m_i} - \frac{Gm_A m_B}{r_{AB}} - Gm_A\sum_{i=1}^{N}\frac{m_i}{r_{iA}}$$
$$- Gm_B\sum_{i=1}^{N}\frac{m_i}{r_{iB}} - G\sum_{i=1}^{N}\sum_{j>i}\frac{m_i m_j}{r_{ij}}, \quad (8)$$

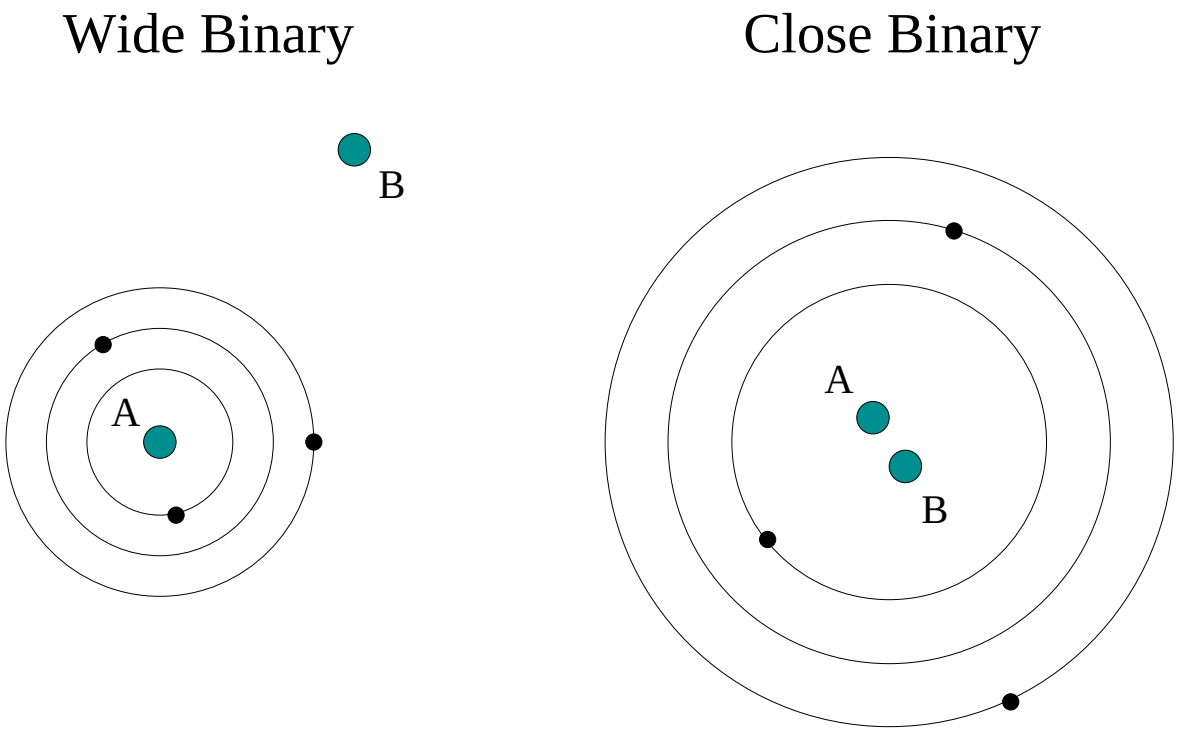

Fig. 1.— Possible configurations of long-lived planetary orbits in binary star systems, where "A" and "B" indicate the two stars in each case.

where A is the central star around which the planets orbit, B is the distant star, and the planets have indices running from 1 to N (see Figure 1). Note that there is no restriction on the relative masses of the two stars.

Making use of the hierarchical arrangement of the binary system, we define a new set of coordinates $\mathbf{R}$ as follows:

$$\begin{aligned} \mathbf{R}_A &= \left(\frac{m_A \mathbf{r}_A + m_B \mathbf{r}_B + \sum_j m_j \mathbf{r}_j}{m_{\rm tot}} \right), \\ \mathbf{R}_i &= \mathbf{r}_i - \mathbf{r}_A, \\ \mathbf{R}_B &= \mathbf{r}_B - \left(\frac{m_A \mathbf{r}_A + \sum_j m_j \mathbf{r}_j}{m_A + \sum_j m_j} \right), \end{aligned} \tag{9}$$

where $m_{tot} = m_A + m_B + \sum_j m_j$ is the total mass of the system, and the summations run from 1 to N. Using these coordinates, the position of each planet is measured with respect to its primary star, while the position of the distant star is measured with respect to the center of mass of all the other objects.

The conjugate momenta $\mathbf{P}$ of these coordinates are

$$\begin{aligned}
\mathbf{P}_A &= \mathbf{p}_A + \mathbf{p}_B + \sum_{j=1}^{N} \mathbf{p}_j, \\
\mathbf{P}_i &= \mathbf{p}_i - m_i \left(\frac{\mathbf{p}_A + \sum_j \mathbf{p}_j}{m_A + \sum_j m_j} \right), \\
\mathbf{P}_B &= \mathbf{p}_B - m_B \left(\frac{\mathbf{p}_A + \mathbf{p}_B + \sum_j \mathbf{p}_j}{m_{\rm tot}} \right),
\end{aligned} \tag{10}$$

where the summations again run from 1 to N.

Expressed in terms of the new coordinates, the Hamiltonian becomes

$$H = H_{\rm Kep} + H_{\rm Int} + H_{\rm Jump}, \tag{11}$$

where

$$\begin{aligned}
H_{\rm Kep} &= \left(\frac{P_B^2}{2\mu_{\rm bin}} - \frac{G m_{\rm tot} \mu_{\rm bin}}{R_B} \right) + \sum_{i=1}^{N} \left(\frac{P_i^2}{2m_i} - \frac{G m_A m_i}{R_i} \right), \\
H_{\rm Int} &= -\sum_{i=1}^{N} \sum_{j>i} \frac{G m_i m_j}{R_{ij}} + G m_B m_A \left(\frac{1}{R_B} - \frac{1}{|\mathbf{R}_B + \mathbf{S}|} \right) \\
&+ G m_B \sum_{i=1}^{N} m_i \left(\frac{1}{R_B} - \frac{1}{|\mathbf{R}_B - \mathbf{R}_i + \mathbf{S}|} \right), \\
H_{\rm Jump} &= \frac{|\sum_{i=1}^{N} \mathbf{P}_i|^2}{2m_A},
\end{aligned} \tag{12}$$

where $\mu_{\rm bin} = (m_A + \sum m_i) m_B / m_{\rm tot}$ is the reduced mass of the binary system (including the mass of the planets), and

$$\mathbf{S} = \frac{\sum_{i=1}^{N} m_i \mathbf{R}_i}{m_A + \sum_{i=1}^{N} m} \tag{13}$$

Note that in deriving these equations, we have added and subtracted terms proportional to $1/R_B$ when splitting the pieces of the Hamiltonian.

The terms in $H_{\rm Kep}$ correspond to the Keplerian motion of the binary star orbit (including the masses of the planets), and the Keplerian motions of the planets about their central star. The terms in $H_{\rm Int}$ are the interactions between planets, and tidal perturbations on the planets due to the distant star. Finally, $H_{\rm Jump}$ contains indirect correction terms. When $H_{\rm Jump}$ is applied, the velocities of the planets remain constant, but the coordinates of each are displaced by a small amount which is proportional to the velocity of the central star.

Note that, in the absence of close encounters, all the terms in $H_{\rm Int}$ and $H_{\rm Jump}$ are small compared to $H_{\rm Kep}$. In addition, each piece of the Hamiltonian can be advanced

efficiently using analytic solutions. Close encounters between planets can be incorporated in a straightforward way by partitioning the planet-interactions terms between $H_{\rm Kep}$ and $H_{\rm Int}$ as in Eq. 7.

In general, one step of the wide-binary integrator consists of 5 substeps:

- Advance $H_{\rm Int}$ for $\tau/2$, where τ is the timestep.
- Advance $H_{\rm Jump}$ for $\tau/2$.
- Advance $H_{\rm Kep}$ for τ.
- Advance $H_{\rm Jump}$ for $\tau/2$.
- Advance $H_{\rm Int}$ for $\tau/2$.

Note that the first and last substeps can be combined into a single substep except at the beginning of the integration or when output is required.

3.2. Close Binary

In a close binary, two stars orbit with a separation which is of the same order as the physical diameters of the stars. In this case, there is unlikely to be room for stable planets to orbit only one member of the binary. However, planetary orbits around the pair of stars can be stable (Holman and Wiegert 1999). The Hamiltonian for N planets in such a system is the same as Eq. 8, except that now A and B refer to two stars lying interior to the planetary orbits.

Using the hierarchical nature of the system, we define a new set of coordinates $\mathbf{R}$ as follows

$$\begin{aligned} \mathbf{R_A} &= \frac{m_A\mathbf{r}_A + \sum m_j\mathbf{r}_j + m_B\mathbf{r}_B}{m_{\rm tot}}, \\ \mathbf{R_i} &= \mathbf{r}_i - \left(\frac{m_A\mathbf{r}_A + m_B\mathbf{r}_B}{m_{\rm bin}}\right), \\ \mathbf{R_B} &= \mathbf{r}_B - \mathbf{r}_A, \end{aligned} \tag{14}$$

where $m_{\rm bin} = m_A + m_B$ is the mass of the binary, $m_{\rm tot}$ is the total mass of the system, and the summations run from 1 to N. Using these coordinates, the position of each planet is measured with respect to the center of mass of the two stars, while R_B gives the relative position of the stars in the binary.

The conjugate momenta P of these coordinates are

$$\begin{aligned}
\mathbf{P}_A &= \mathbf{p}_A + \mathbf{p}_B + \sum_{j=1}^{N} \mathbf{p}_j, \\
\mathbf{P}_i &= \mathbf{p}_i - m_i \left(\frac{\mathbf{p}_A + \mathbf{p}_B + \sum_j \mathbf{p}_j}{m_{\rm tot}} \right), \\
\mathbf{P}_B &= \mathbf{p_B} - m_B \left(\frac{\mathbf{p}_A + \mathbf{p}_B}{m_{\rm bin}} \right),
\end{aligned} \tag{15}$$

where the summation indices run from 1 to N.

Expressed in terms of the new coordinates, the Hamiltonian becomes

$$H = H_{\rm Kep} + H_{\rm Int} + H_{\rm Jump}, \tag{16}$$

where

$$\begin{aligned}
H_{\rm Kep} &= \left[\frac{P_B^2}{2\mu_{\rm bin}} - \frac{G m_{\rm bin} \mu_{\rm bin}}{R_B} \right] + \sum_{i=1}^{N} \left[\frac{P_i^2}{2m_i} - \frac{G m_{\rm bin} m_i}{R_i} \right], \\
H_{\rm Int} &= G m_{\rm bin} \sum_{i=1}^{N} m_i \left[\frac{1}{R_i} - \frac{m_A}{|m_{\rm bin}\mathbf{R}_i + m_B \mathbf{R}_B|} - \frac{m_B}{|m_{\rm bin}\mathbf{R}_i - m_A \mathbf{R}_B|} \right], \\
&- \sum_{i=1}^{N} \sum_{j>i} \frac{G m_i m_j}{R_{ij}} \\
H_{\rm Jump} &= \frac{|\sum_{i=1}^{N} \mathbf{P}_i|^2}{2m_{\rm bin}},
\end{aligned} \tag{17}$$

where $\mu_{\rm bin} = m_A m_B/(m_A + m_B)$ is the reduced mass of the binary star.

The terms in $H_{\rm Kep}$ correspond to the Keplerian motion of the binary stars about one another, and of the planets about the center of mass of the binary. The terms in $H_{\rm Int}$ are the interactions between planets, and perturbations on the planets due to the higher order moments of the binary's potential. Finally, $H_{\rm Jump}$ contains indirect correction terms.

In the absence of close encounters, all the terms in $H_{\rm Int}$ and $H_{\rm Jump}$ are small compared to $H_{\rm Kep}$, and each part of the Hamiltonian can be advanced analytically. Close encounters between planets can be incorporated as before by partitioning the planet-interactions terms between $H_{\rm Kep}$ and $H_{\rm Int}$ as in Eq. 7.

In general, one step of the close-binary integrator consists of 5 substeps, similar to those for the wide-binary integrator. However, in this case the timestep must be small in order to integrate the orbit of the binary star. A more efficient scheme is to assign a separate small timestep $\tau/N_{\rm bin}$ to the binary star, while choosing a larger global timestep τ to integrate the planets. (This procedure is similar to that used by Saha and Tremaine 1994.) In practice, we do this by splitting $H_{\rm Kep}$ into a piece $H_{\rm BKep}$ that involves terms in

$\mathbf{R}_B$ and $\mathbf{P}_B$ and a piece $H_{\rm PKep}$ that does not. Similarly, we split $H_{\rm Int}$ into 2 new parts $H_{\rm BInt}$ and $H_{\rm PInt}$.

$$\begin{aligned}
H_{\rm BKep} &= \frac{P_B^2}{2\mu_{\rm bin}} - \frac{Gm_{\rm bin}\mu_{\rm bin}}{R_B}, \\
H_{\rm PKep} &= \sum_{i=1}^{N} \left[\frac{P_i^2}{2m_i} - \frac{Gm_{\rm bin}m_i}{R_i} \right], \\
H_{\rm BInt} &= Gm_{\rm bin} \sum_{i=1}^{N} m_i \left[\frac{1}{R_i} - \frac{m_A}{|m_{\rm bin}\mathbf{R}_i + m_B\mathbf{R}_B|} - \frac{m_B}{|m_{\rm bin}\mathbf{R}_i - m_A\mathbf{R}_B|} \right], \\
H_{\rm PInt} &= -\sum_{i=1}^{N} \sum_{j>i} \frac{Gm_im_j}{R_{ij}}.
\end{aligned} \tag{18}$$

One timestep of the close-binary integrator now looks like:

- Advance $H_{\rm PInt}$ for $\tau/2$, where τ is the timestep.
- Repeat the following $N_{\rm bin}$ times:
  - Advance $H_{\rm BInt}$ for $\tau/(2N_{\rm bin})$.
  - Advance $H_{\rm BKep}$ for $\tau/(2N_{\rm bin})$.
- Advance $H_{\rm Jump}$ for $\tau/2$.
- Advance $H_{\rm PKep}$ for τ.
- Advance $H_{\rm Jump}$ for $\tau/2$.
- Repeat the following $N_{\rm bin}$ times:
  - Advance $H_{\rm BKep}$ for $\tau/(2N_{\rm bin})$.
  - Advance $H_{\rm BInt}$ for $\tau/(2N_{\rm bin})$.
- Advance $H_{\rm PInt}$ for $\tau/2$.

In our implementation, we make $N_{\rm bin}$ approximately equal to the ratio of the orbital period of the innermost planet to that of the binary, although this may not be the optimal choice. Note that we could also use independent timesteps for the binary and the planets in the wide-binary algorithm described in Section 3.1. However, in this case the amount of computer time saved would be modest since most of the expense is required to calculate the direct perturbations between the planets, and the basic algorithm already uses an optimal timestep for this.

4. Tests

In this section we describe some tests we have made using the new symplectic algorithms.

4.1. Conservation of Jacobi Constant

As a first test of the new algorithms we examined the restricted three-body problem. We integrated the orbits of test particles moving in the orbital plane of two stars with masses m_A and m_B. The stars themselves moved on circular orbits about one another. The restricted problem has an integral of the motion, the Jacobi constant C, given by

$$C = \frac{1}{2}(\dot{x}^2 + \dot{y}^2) - \frac{Gm_A}{\Delta_A} - \frac{Gm_B}{\Delta_B} - n(x\dot{y} - y\dot{x}), \tag{19}$$

where $\mathbf{r}$ and $\dot{\mathbf{r}}$ are the barycentric coordinates and velocities of the test particle, Δ_A and Δ_B are the distances of the particle from the two stars respectively and $n^2a^3 = G(m_A + m_B)$, where a is the semi-major axis of the binary orbit.

We integrated 8 test particles in a close-binary system and another 8 in a wide-binary system, with $m_A = m_B = 1$ $M_\odot$ in each case. All of the test particles initially had semi-major axes of 1 AU, and circular orbits. The initial longitudes of the particles were spaced at intervals of 45°. The close binary star had $a = 0.25$ AU and a period of 32.3 days, while the wide binary system had $a = 4$ AU and a period of 2070 days. The particles in these systems have orbits that appear to be stable, but they lie close to the critical semi-major axis at which they would be unstable. The integrations used a timestep of 7 days, with $N_{\rm bin} = 8$ for the binary star in the close binary system. Each integration lasted for 1 million years.

Figure 2 shows the relative error in the Jacobi constant for two typical particles in each integration. In each case, the relative error oscillates with an amplitude of order 1 part in 10000, with the close-binary algorithm slightly more accurate than the wide-binary one. In addition, there is no secular trend in the errors with time, which is typical of symplectic methods. For comparison, the two rightmost panels of Figure 2 show the result of integrating the wide-binary system using a standard hybrid symplectic integrator (Chambers 1999) with a timestep of 7 days. This algorithm is not designed for systems containing two very massive bodies, and the errors in the particles' Jacobi constants are larger by an order of magnitude.

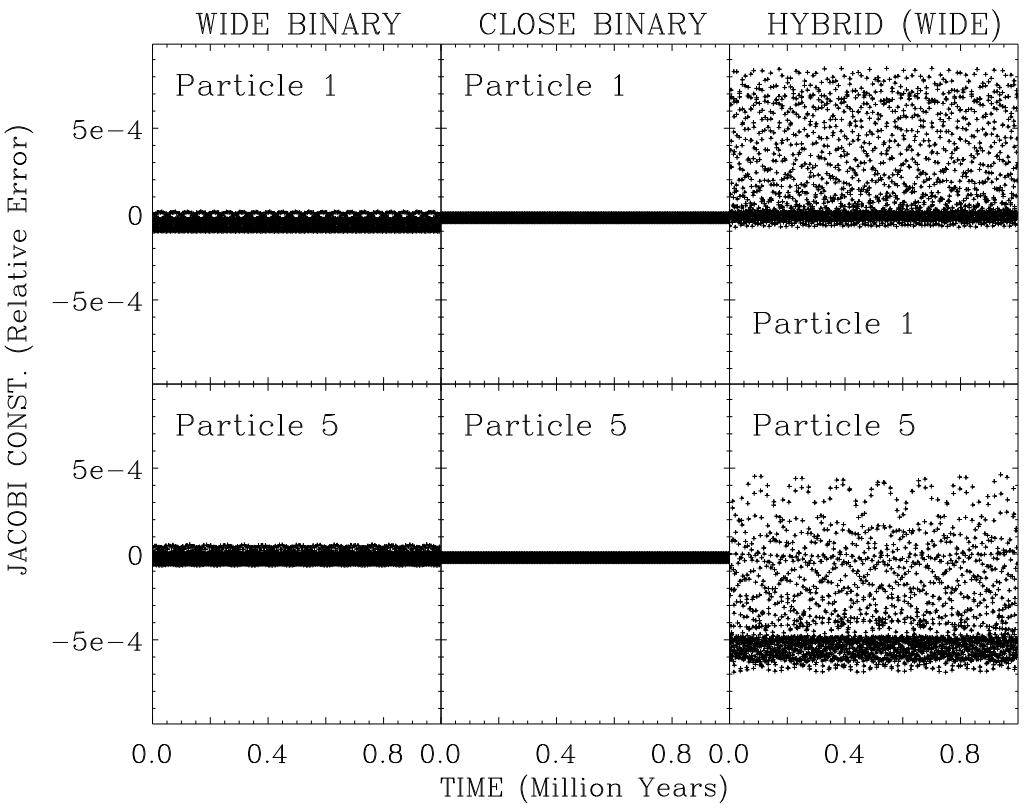

Fig. 2.— Relative error of the Jacobi constant for particles orbiting a wide binary and a close binary, using the algorithms described in this paper. Also shown is an integration of the wide-binary system using a hybrid symplectic integrator.

4.2. Tests Particles Orbiting α Centauri

Wiegert and Holman (1997) made a detailed survey of the stability of test particles orbiting the α Centauri binary star system. This system contains two stars of mass 1.1 and 0.91 $M_\odot$ moving on an orbit with semi-major axis 23.4 AU, and eccentricity 0.52. The authors used the symplectic integrator of Wisdom and Holman (1991) to determine the maximum semi-major axis, $a_{\rm crit}$ below which all orbits around the primary star are stable, as a function of the particles' inclination, i, relative to the binary orbit. In the zero inclination case, $a_{\rm crit}$ is about 0.1 times the binary semi-major axis. The authors found that $a_{\rm crit}$ is a strong function of the test particles' inclination, reaching a minimum of close to zero for $i = 90°$.

Here, we have reproduced this test using the wide-binary integration algorithm described above. We integrated 13 sets of 50 test particles with initially circular orbits about the primary star, with semi-major axes $0.23 \leq a \leq 11.5$ AU, spaced at intervals of

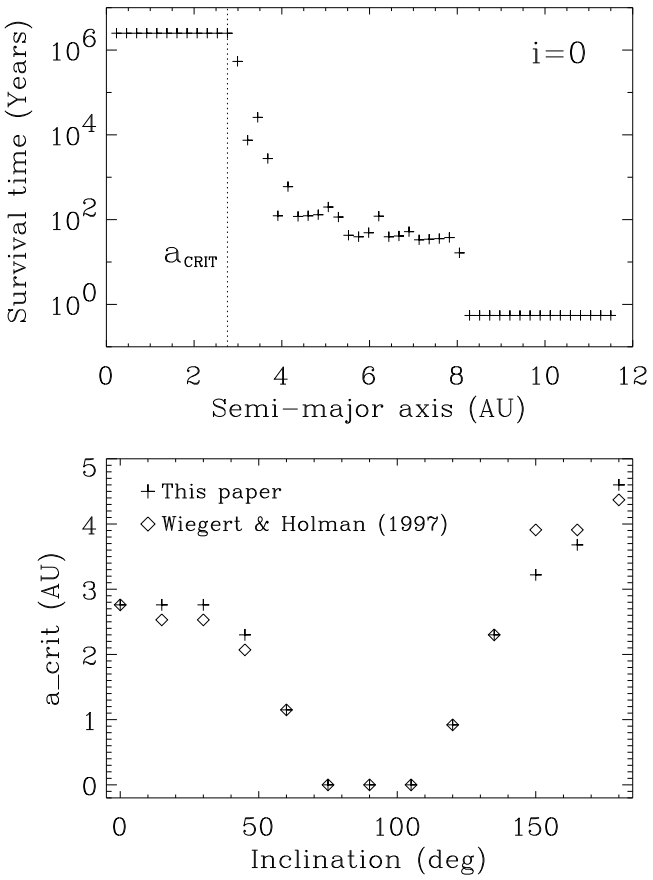

Fig. 3.— Upper: survival time of particles orbiting the primary of the α Cen. binary as a function of their initial semi-major axis (zero-inclination case). Lower: Critical semi-major axis for such particles as a function of their initial inclination.

0.23 AU. Each set of particles began with a different initial inclination relative to the binary orbit. We examined cases with relative inclinations $0 \leq i \leq 180°$, spaced at intervals of 15°. In each integration, the secondary star was started at apoastron, on the opposite side of the primary from the test particles. The integrations lasted for 2.5 million years, and the integrator used a stepsize of 2 days. Particles were deemed to be unstable if their distance from the primary became greater than the semi-major axis of the binary or less than 0.0234 AU.

The upper panel of Fig. 3 shows the lifetime of particles in the zero-inclination case as a function of their initial semi-major axis a. Test particles with $a > 8$ AU became unstable almost immediately after the start of the integration. Particles with $3 < a < 8$ AU survived longer, but ultimately became unstable, with the time required to become unstable generally increasing as a decreased. In this simulation, all particles with $a \leq 2.76$

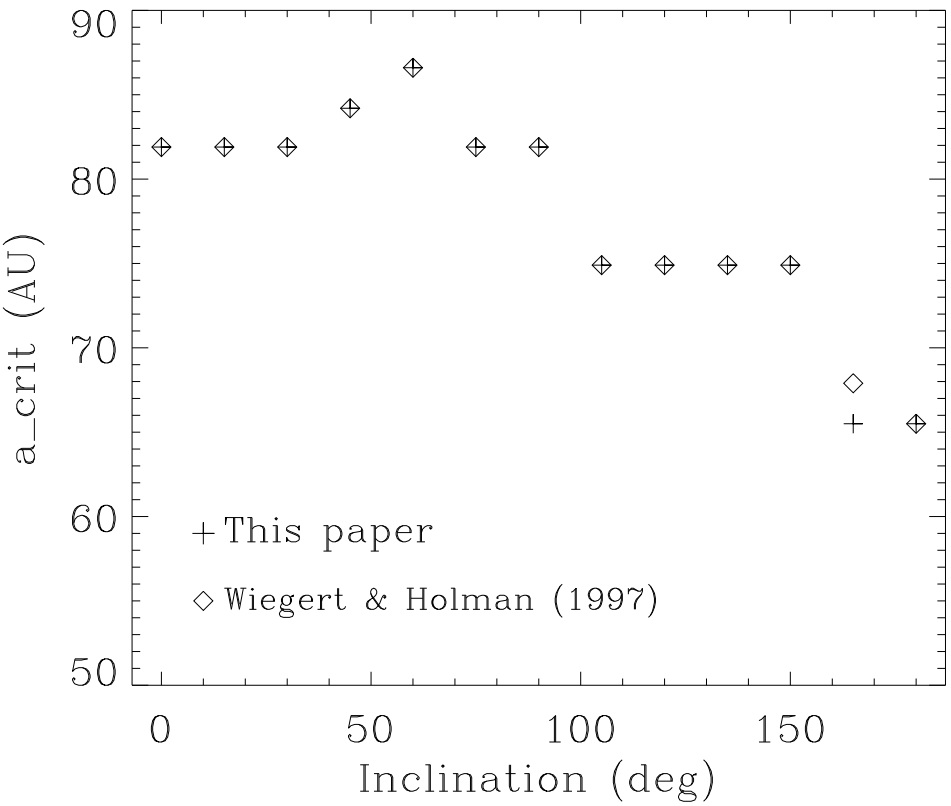

Fig. 4.— Critical semi-major axis for particles orbiting both members of the α Cen. binary, as a function of their initial inclination.

AU remained stable throughout the integration, which agrees with the result of Wiegert and Holman (1997). This is indicated by the line labelled $a_{\rm crit}$ in the upper panel of Fig. 3. However, we note that some of the particles with $a < 2.76$ AU may prove to be unstable on longer timescales.

The lower panel of Fig. 3 shows the critical semi-major axis as a function of initial inclination, in our integrations and those of Wiegert and Holman (1997). In general, the agreement is good, although in some cases, particles are found to be unstable in one of the simulations but not the other. We suggest that these particles will ultimately prove to be unstable using both integration techniques if integrated for long enough. However, the time required for a particular particle to become unstable appears to depend sensitively on the integrator used. The fact that the results are similar using the two algorithms, with no systematic differences, gives us confidence that our new algorithm works.

Wiegert and Holman (1997) also looked at test particles orbiting both members of the α Cen. binary, and we have reproduced that test using the close-binary algorithm described in Section 3.2. We integrated 13 sets of particles with initially circular orbits

about the barycenter of the binary. Particles within each set began with semi-major axes $35.1 < a < 117$ AU, spaced at intervals of 2.34 AU. Each set of particles began with a single inclination relative to the binary, with $0 \leq i \leq 180°$ for different sets, spaced at intervals of 15°. In each integration, the secondary star was started at apoastron, on the opposite side of the primary to the test particles. The integrations lasted for 2.5 million years, using an integrator stepsize of 100 days with $N_{\rm bin} = 2$. Particles were removed if their distance from the primary became less than 23.4 AU or more than 20000 AU.

Figure 4 shows the critical semi-major axis $a_{\rm crit}$ for these simulations as a function of the initial inclination. Here we define $a_{\rm crit}$ to be the minimum semi-major axis above which all the particles appear to be stable. The figure also shows the results obtained by Wiegert and Holman (1997). We note that, in common with Wiegert and Holman, we have described a particle as "unstable" if its time-averaged semi-major axis differed by more than 5% from its initial value. These particles are likely to be removed by a close encounter or ejection on timescales longer than our integration. The results in Fig. 4 using the binary code are almost identical to those of Wiegert and Holman (1997), with $a_{\rm crit}$ differing at only one value of i.

4.3. Close Stellar Passage

Ida *et al.* (2000) have investigated the effect of the passage of a star on a nearly parabolic orbit passing just outside the primordial Edgeworth-Kuiper belt. These authors found that the degree to which the orbits of objects in the belt were perturbed depended strongly on an object's semi-major axis in units of the star's perihelion distance.

We have reproduced one of their calculations using the wide-binary algorithm described in Section 3.1. We integrated 760 test particles, with initially circular, coplanar orbits, and semi-major axes $5 < a < 80$ AU, for 20000 years. The particles began orbiting a 1 $M_\odot$ star, while a second 1 $M_\odot$ star moved on a parabolic orbit, inclined at 30°, with a periapse distance of 100 AU, passing through periapse midway through the integration. The test particles were grouped into batches of 10, each batch having the same initial a, spaced at intervals of 1 AU. Within each batch, the initial longitudes were spaced at intervals of 36°.

Figure 5 shows the final distributions of e and i for the test particles as a function of the final values of a, where a is measured in units of the binary periapse distance q. The distributions are divided into two regimes. For small values of a, the degree of excitation of e and i is a power-law function of the semi-major axis. In this regime, e and i are approximately proportional to $(a/q)^{5/2}$ and $(a/q)^{3/2}$ respectively. At larger values of a, the degree of excitation is larger, and also depends on the initial longitudes of the particles due to the effect of mean-motion resonances. These characteristics, and the distributions themselves are essentially identical to those of Fig. 2b of Ida *et al.* (2000).

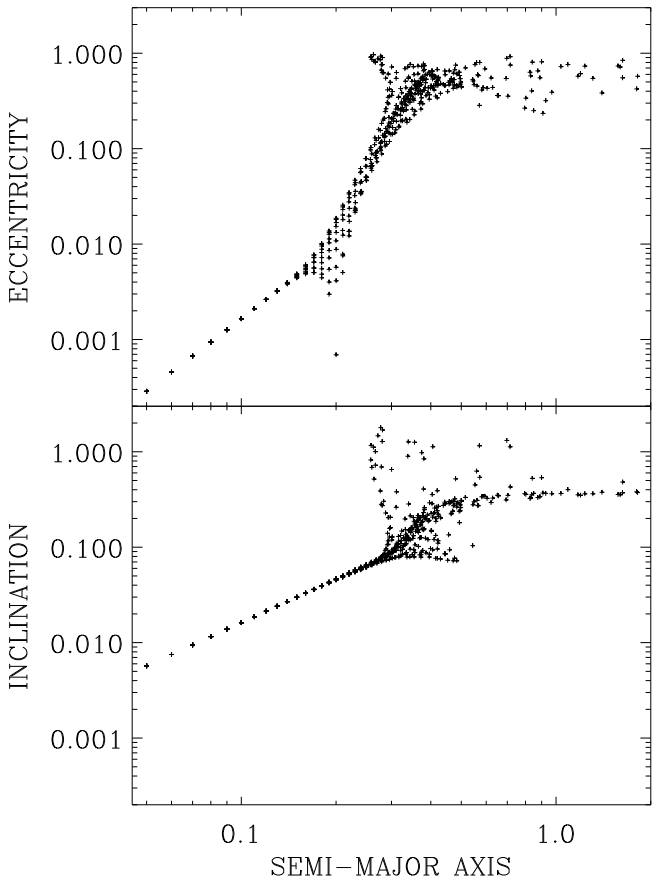

Fig. 5.— Final eccentricity e and inclination i versus final semi-major axis a for 750 test particles following the passage of a 1 $M_\odot$ star on a parabolic orbit with $i = 30°$. Initially $e = i = 0$ for all particles; a is in units of the star's perihelion distance, i is in radians.

4.4. Evolution of a System of Giant Planets

The tests described above have all involved massless test particles. In this section, we describe a test involving a system of massive bodies. The system consists of 3 giant planets with initial orbits identical to those of Jupiter, Saturn and Uranus, with the masses of all 3 planets set equal to that of Jupiter. We integrated this system using both of the binary algorithms and also a symplectic code that included a symplectic corrector (Wisdom *et al.* 1996). For the close-binary code, we designated Sun and Jupiter as the binary system orbited by the other 2 planets. For the wide-binary case, the mass-enhanced Uranus played the role of a distant binary companion and the other 2 planets were assumed to orbit the Sun. Each of these approximations is reasonable, although a true hierarchical system is a better approximation still. For this reason we compared the results using the binary codes

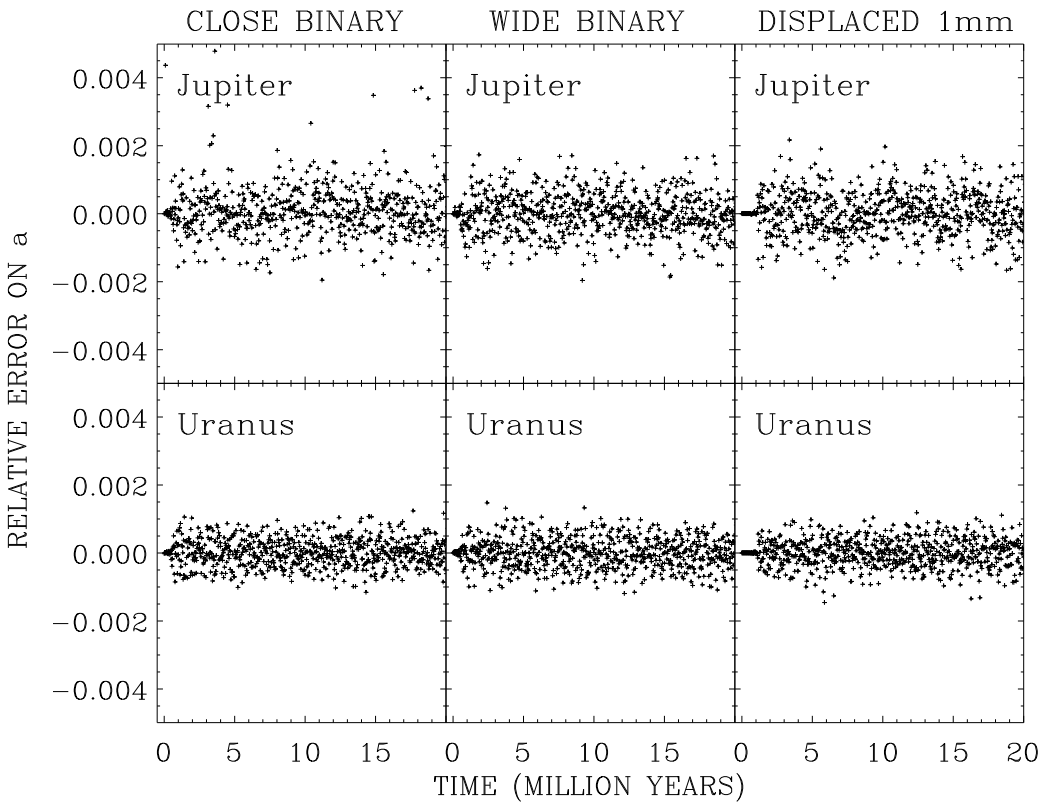

Fig. 6.— Relative error on the semi-major axes of Jupiter and Neptune integrated for 20 million years using the close and wide-binary algorithms. Also shown is the difference between 2 integrations using a standard scheme (including a symplectic corrector) in which the innermost planet was initially displaced by 10^{-14} AU.

with a reference integration which used a conventional symplectic integrator using Jacobi coordinates. This integrator also included a simple symplectic corrector to increase the accuracy of the reference calculation. Note that each of the calculations integrated the same system of 4 bodies. The only difference is in the method of integration.

The calculations ran for 100 million years using a stepsize of 50 days (100 days for the close binary algorithm, with $N_{\rm bin} = 2$). Initial data for the planets were taken from JPL ephemeris DE200. Figure 6 shows the relative error on the Jacobi semi-major axes of Jupiter and Uranus for the first 20 million years of the integrations (the remainders of the simulations are similar). For each of the binary codes, the errors are calculated by comparing the results with the reference integration. The latter had an energy error of about 1 part in 10^{10} at the end of the integration, compared to about 1 part in 10^7 for the binary codes. This difference is due mostly to the incorporation of a symplectic corrector

in the standard code. (Note that a corrector could be applied to the binary algorithms, but our purpose here is to compare the basic binary algorithms with a more accurate integration.)

The relative errors in a are typically about one part in 1000 for both Jupiter and Uranus, centered on zero, with no secular trend towards larger or smaller values of a. In the each case, the relative error exhibits high frequency oscillations, but the envelope encompassing these oscillations does not grow with time. These properties are typical of symplectic algorithms. The errors are comparable to the typical relative change in a for either planet on timescales of an orbital period, which suggests that the differences are due to errors in the phases rather than the actions.

As an additional test, we reran the reference calculation displacing the initial orbit of the innermost planet by 10^{-14} AU. The difference between the 2 reference integrations is shown in the rightmost panels of Fig. 6. These integrations diverged rapidly, suggesting that this system is highly chaotic with a Lyapunov time $\sim 50,000$ years. After 1.5 million years, the difference between the reference calculations was comparable to the difference of either from the binary integrations suggesting that the binary algorithms do a good job of following the evolution of systems involving massive bodies on long timescales.

4.5. Planetary Accretion

As a final test of the wide-binary algorithm, we present some N-body accretion calculations designed to simulate the final stage of the formation of the terrestrial planets. These calculations include many close encounters, and so they provide a test of the combination of the binary coordinate system with the hybrid method for dealing with close encounters.

Our reference calculation was an accretion integration taken from Chambers (2001), which used a hybrid symplectic integrator. The simulation began with 154 embryos with initial semi-major axes $0.3 < a < 2.0$ AU, eccentricities $0 < e < 0.01$ and inclinations $0 < i < 0.5°$. Fourteen of the embryos began with a mass similar to Mars, and the remaining 140 had masses comparable to the Moon. Collisions between pairs of bodies resulted in a simple merger, conserving mass and momentum. The integration also included Jupiter, starting with its current mass and orbital elements.

We redid this calculation twice using the wide-binary algorithm, with Jupiter as the distant binary member. One calculation (Run 1) began with identical initial conditions to that of Chambers (2001). In the second calculation (Run 2), we moved the initial position of one of the smaller embryos by 1 meter along its orbit, leaving all other initial conditions unchanged. N-body planetary accretion simulations are known to be highly stochastic (*e.g.*, Chambers and Wetherill 1998), so we anticipated that the two integrations using the wide-binary code would diverge and give different results. Making two calculations

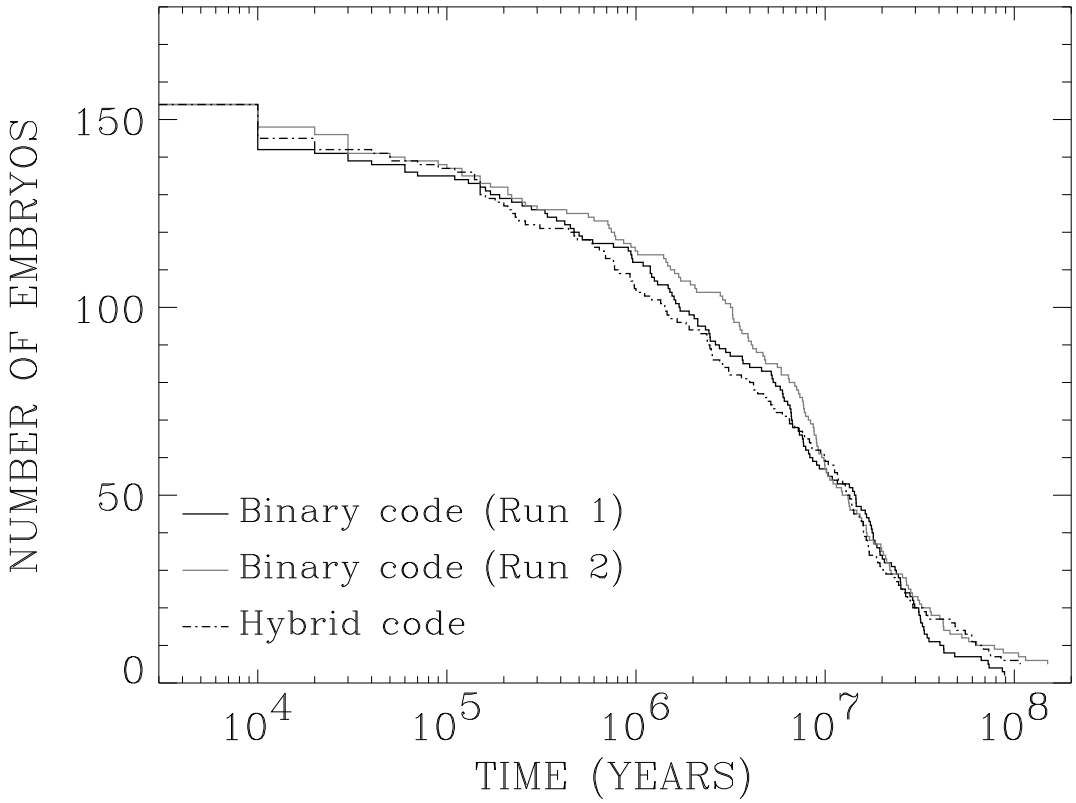

Fig. 7.— Number of surviving embryos versus time for N-body accretion integrations of 154 planetary embryos, plus Jupiter, integrated using the wide-binary code and a hybrid symplectic code. Run 2 is identical to Run 1 except that one embryo was initially displaced by 1 meter.

with almost identical initial conditions allows us to compare differences caused by using different integration algorithms with those caused by the inherently chaotic nature of such calculations.

Figure 7 shows the number of remaining embryos N versus time in the 3 integrations. The values of N diverge almost immediately, emphasizing the degree to which such calculations are chaotic. However, N decreases in a similar manner for each integration, implying that the accretion rates were similar. In particular, the difference between the results of the two simulations using the wide-binary code is comparable to the difference of either simulation from the results using the hybrid code. This suggests that the binary algorithm is working well in this case. The two simulations using the binary code ended with 2 and 5 final planets respectively, while the hybrid-code simulation produced 4 final planets. The striking difference between the binary-code simulations, despite using almost

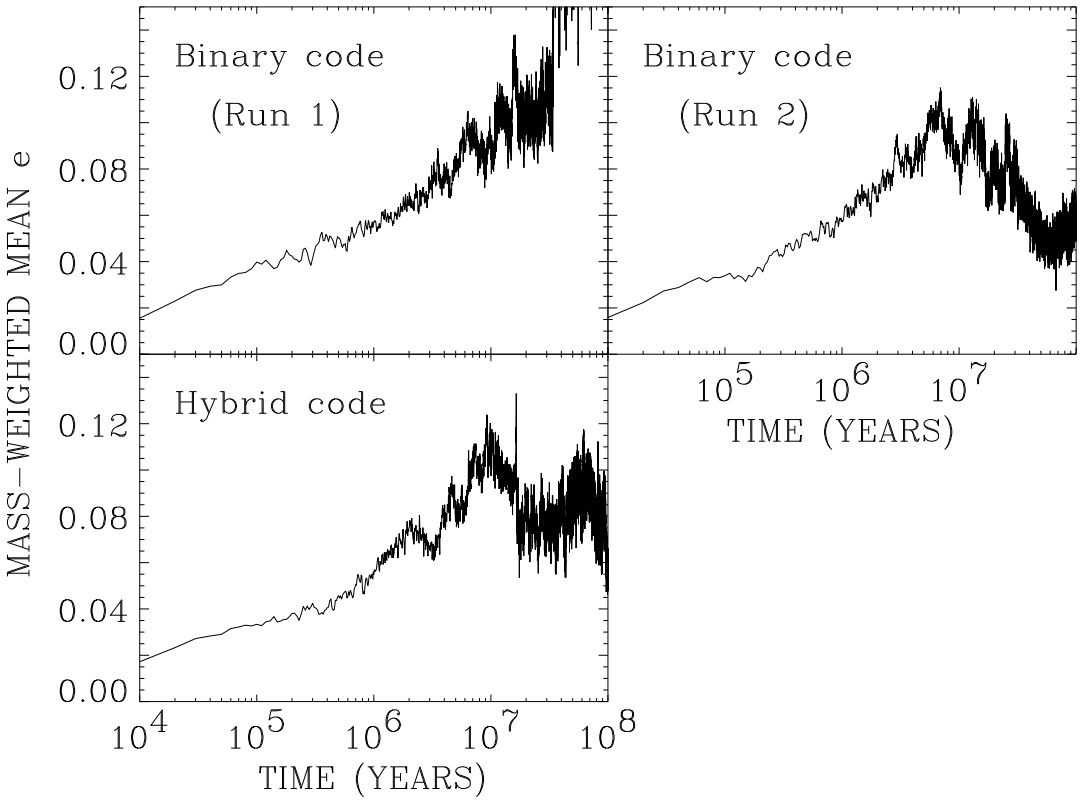

Fig. 8.— Mass-weighted mean eccentricity for N-body accretion integrations of 154 planetary embryos, plus Jupiter, integrated using the wide-binary code and a hybrid symplectic code. Run 2 is identical to Run 1, except that one embryo was initially displaced by 1 meter.

identical initial conditions, emphasizes the chaotic nature of such calculations.

Figure 8 shows the mass-weighted mean eccentricity $\bar{e}$ for surviving embryos versus time in the 3 simulations. The embryos began with nearly circular orbits, and their eccentricities typically increased over time due to close encounters and secular perturbations. The graphs differ from one another almost from the start of the calculations. However, in each case, $\bar{e}$ increased for the first 10^7 years of the simulation, roughly linearly in log time, to a value of roughly 0.1. At this point, the number of embryos remaining was quite small, and the simulations diverged qualitatively, with the hybrid case lying roughly in between the two simulations using the binary code. The differences between the integrations using the binary code are again comparable to the difference of either from the integration using the hybrid, which suggests that the binary code is suitable for accretion calculations.

5. Summary

In this paper we have devised and tested two new symplectic integration algorithms appropriate for N-body problems in binary star systems. The new codes follow close encounters accurately, and so they can be used to make N-body simulations of planetary accretion in binary systems. Each algorithm uses a new set of coordinates that reflects the hierarchical nature of stable planetary orbits in binary star systems, with one coordinate set appropriate for planets orbiting a single star, and the other appropriate for planets orbiting both stars. If desired, the method used to derive these algorithms could be extended to consider planets orbiting each of the stars in a binary, or planetary orbits in hierarchical multiple-star systems.

JEC wishes to thank NRC for primary support, in addition to DENI, PPARC and Starlink. MJD is grateful for the continuing financial support of the National Sciences and Engineering Research Council of Canada. This work was supported in part by NASA's Origins of Solar Systems Research Program through grant NAG5-9680 and a NASA Graduate Student Researchers Program Fellowship awarded to EVQ.

REFERENCES

Canup, R.M., Levison, H.F. and Stewart, G.R., 1999, AJ, 117, 603

Chambers, J.E. 2001, Icarus, 152, 205

Chambers, J.E. 1999, MNRAS, 304, 793

Chambers, J.E. and Wetherill, G.W., 1998, Icarus, 136, 304

Cochran, D.C., Hatzes, A.P., Butler, R.P. and Marcy, G.W. 1997, ApJ, 483, 457

Duncan, M.J., Levison, H.F., and Lee, M.H. 1998, AJ, 116, 2067

Everhart E., 1985, in Carusi A., Valsecchi G.B., ed., Dynamics of Comets: Their Origin and Evolution. Reidel, p. 185

Holman M.J. and Wiegert P.A. 1999. AJ, 117, 621

Ida A., Larwood, J. and Burkert, A., ApJ, 528, 351

Kinoshita, H., Yoshida, H. and Nakai, H. 1991, Cel. Mech. Dyn. Astron., 50, 59

Levison, H.F. and Duncan, M.J., 1994, Icarus, 108, 18

Rivera, E.J. and Lissauer, J.J, 2000, ApJ, 530, 454

Saha P. and Tremaine S., 1992, AJ, 104, 1633

Saha P. and Tremaine S., 1994, AJ, 108, 1962

Stoer J., Bulirsch R., 1980, Introduction to Numerical Analysis. Springer-Verlag, New York

Wiegert, P.A. and Holman, M.J. 1997, AJ, 113, 1445

Wisdom, J. and Holman, M. 1991, AJ, 102, 1528

Wisdom, J., Holman, M. and Touma, J., Fields Inst. Comm., 10, 217

This manuscript was prepared with the AAS LaTeX macros v4.0.